*Refereed Proceedings*

*Heat Exchanger Fouling and Cleaning: Fundamentals and Applications*

Engineering Conferences International *Year* 2003

# Fouling Characteristics of a Light Australian Crude Oil

Zaid S. Saleh* R. Sheikholeslami†

A. P. Watkinson‡

*The University of New South Wales

†The University of New South Wales

‡The University of British Columbia

# Fouling Characteristics of A Light Australian Crude Oil

**Zaid S. Saleh[1], R. Sheikholeslami[1] and A.P. Watkinson[2]**

[1]Department of Chemical Engineering and Industrial Chemistry,
The University of New South Wales, Sydney, NSW 2052, Australia.
[2]Department of Chemical and Biological Engineering,
The University of British Columbia, Vancouver, B.C., V6T 1Z4, Canada

## ABSTRACT

Australian crude oils, which generally contain little asphaltenes, nevertheless give rise to fouling in refinery pre-heat trains. In this research, fouling of a series of such crude oils and their blends is being assessed. The present work focuses on thermal fouling resulting from heating Gippsland crude oil at moderate temperatures. The oil is maintained under nitrogen at a pressure of 379 kPa, and re-circulated at bulk temperatures of 80-120$^{o}$C through an electrically heated annular probe at velocities in the range 0.25 to 0.65 m/s with surface temperatures from 180-260°C. Experiments are run for periods up to 90 hours at constant heat flux. Fouling is detected by the increase of wall temperature of the probe.

The oil is characterized by its filterable solids content, density and viscosity both before and after the fouling run. The trends in fouling rates are compared to predictions of the threshold-fouling model proposed by Ebert and Panchal (1995). Data on deposit composition are presented, and the fouling mechanism discussed.

## 1. INTRODUCTION

The term fouling is defined as the deposition of unwanted materials on heat transfer equipment, which results in an increase in thermal resistance to heat transfer and subsequent loss of the equipment thermal efficiency. The growth of deposits causes the thermal hydraulic performance of heat transfer equipment to decrease continuously with time. This fouling problem remains a major cost penalty in oil refineries costing millions of dollars every year (Bott, 1995).

Crude oil fouling is generally believed to be caused by impurities in the crude oil such as corrosion products, water and salt, by asphaltenes exceeding their solubility limit, or by thermal decomposition or autoxidation of reactive constituents in the oil. Asphaltene precipitation is considered to be a major cause of crude unit fouling. As well, reactive constituents of oil may undergo thermal decomposition, polymerization, or autoxidation reactions to produce fouling precursors or foulants (Murphy and Campbell, 1992). Dickakian (1997) has shown the role of asphaltene and polar molecules in fouling at elevated temperatures where coke is produced following phase separation. At lower temperatures, asphaltenes precipitation occurs due to changes in solvent nature via blending, or pressure change.

Gippsland crude oil produced in Australia gives rise to fouling problems in refineries operated by Caltex Australia, in spite of its low sulphur, ash and asphaltene levels. Among possible causes of the fouling are precipitation of species resulting from seasonal changes in composition (due to changing temperature or other conditions in storage tanks, pipelines, or refineries), autoxidation leading to gum formation due to oxygen entering the oil in storage, or release of corrosion products from within the production, transportation or processing units which subsequently deposit in the heat exchanger (Lambourn and Durrieu, 1983).

The present work was undertaken to study the effect of fluid properties and operating conditions, with the intention of using the results to guide a fouling mitigation strategy.

## 2. MATERIALS AND METHODS

Table 1 lists the properties of Gippsland crude oil used in the fouling tests. Both asphaltene and sulphur contents are very low. The apparatus consists of a re-circulation loop containing a 10-L feed tank and a pump; an orifice plate was used for flow measurement in conjunction with an annular (HTRI) heat transfer probe, which was operated at constant heat flux with time.

Crude oil was poured into the feed tank, purged with nitrogen and pressurized to 379 kPa. The inlet and outlet bulk temperatures along with the probe surface temperature were measured via thermocouples. The fouling resistance was determined at constant heat flux by the decrease in heat transfer coefficient with time, as is shown below.

Under clean conditions at time zero the reciprocal of the overall coefficient is given by:

$$\frac{1}{Uo} = \frac{(T_s - T_b)_o}{q/A} \quad (1)$$

however, under fouled conditions it is given by:

$$\frac{1}{U(t)} = \frac{(T_s - T_b)_t}{q/A} \quad (2)$$

where $T_s$ is the average surface temperature of the probe measured using thermocouples embedded within the metal surface of the probe heating section. The fouling resistance is calculated using the expression:

$$R_f(t) = \frac{1}{U(t)} - \frac{1}{Uo} = \frac{(T_s - T_b)_t - (T_s - T_b)_o}{q/A} \quad (3)$$

The fouling rate can then be calculated as:

$$\frac{dR_f}{dt} = \frac{d}{dt}\left(\frac{1}{U(t)}\right) \quad (4)$$

Initial fouling rates were determined from the slope of the $R_f$ versus time curves over linear portions, and with due regard for any induction time. The procedure used to determine the end of the induction period is as follows. The total change in (1/U) over the run was determined first. Starting from the beginning of each run, the change in (1/U) is checked for every 10 hr intervals. The time at which the change is 5% or more of the total change in 1/U is taken to be the end of the induction period. The end of the initial fouling rate period was determined by calculating the average change in 1/U over 10 hours, which has to be not less than 2% of the total.

The heat transfer characteristics of the PFRU unit under clean condition were determined using Paraflex, a non fouling solvent. The clean heat transfer coefficients $U_0$, for Paraflex and crude oil, in equation (1) were calculated using a mean surface temperature and expressed as a Nusselt number. Experimental values were compared with predictions of the equation of Gnielinski (1995), in which properties are based on the bulk temperature:

$$Nu = \frac{(\zeta/8)(Re - 1000)\,Pr}{1 + 12.7(\zeta/8)^{0.5}(Pr^{2/3} - 1)}\left(1 + \left(\frac{D}{L}\right)^{2/3}\right)\left(\frac{\mu_b}{\mu_w}\right)^{0.14} \quad (5)$$

$$\zeta = (1.82 \log Re - 1.64)^{-2} \quad (6)$$

where Nu = Nusselt Number = $\frac{U_o d_h}{\lambda}$,

the hydraulic diameter, $d_h = d_{a,o} - d_{a,i} = 14.3$ mm, and L is the length of the heating section = 102 mm.

Table 1. Properties of Gippsland crude oil and Paraflex.

| Property | Gippsland | Paraflex |
|---|---|---|
| Density (g/ml) at 20°C | 0.792 | 0.855 |
| Vapor Pressure(37°C) psi | 5.0 | - |
| Total Sulfur (wt%) | 0.12 | - |
| Total Nitrogen (PPM) | 120 | - |
| Viscosity (mPa.s) at 20°C | 1.969 | 23.9 |
| Water Content (vol%) | 0.01 | - |
| Ash (wt%) | <0.01 | - |
| Asphaltenes (wt%) | 0.05 | - |
| Resin Content (wt%) | 7.2 | - |
| Carbon Content (wt%) | 85.78 | - |
| Hydrogen Content (wt%) | 14.10 | - |
| Pour point (°C) | <-42 | -21 |

The Ebert and Panchal (1995) threshold-fouling model, Eq. 7, was used to compare the trends in fouling rate. This model was originally developed using data on coke deposition from crude oils subject to high heat fluxes.

$$\frac{dR_f}{dt} = \alpha\, Re^{\beta} \exp(-E/RT_f) - \gamma\tau \quad (7)$$

Following an experiment, deposits on the heated section were photographed and collected for chemical and physical characterization (i.e. SEM). The amount of deposit was very small; samples were analyzed by micro-analytical techniques in order to determine deposit chemistry (C, H, N and S).

The presence of any filterable solids in the oil was determined by filtration through a 3 micron membrane filter at 85°C.

## 3. RESULTS AND DISCUSSIONS

Clean heat transfer tests were performed with Paraflex, and the Nusselt numbers compared with the predictions of the aforementioned correlation (Eq. 5). Results are presented in Table 2:

Table 2. Comparison of experimental and predicted Nusselt numbers.

| u (m/s) | Reynolds Number | Nu Gnielinski | Nu Experiment |
|---|---|---|---|
| 0.54 | 2659 | 108 | 145 |
| 0.66 | 3282 | 123 | 160 |
| 0.77 | 3805 | 134 | 170 |
| 0.87 | 4263 | 144 | 181 |
| 0.95 | 4677 | 153 | 191 |
| 1.1 | 5411 | 168 | 203 |
| 1.23 | 6057 | 180 | 218 |

The Gnielinski equation under-predicted the experimental results by a factor of 1.2 to 1.34. Systematic error sources lie in the reliability of the physical property of Paraflex data and the fouling probe itself.

Experiments were carried out to examine the effect of operating conditions on fouling of the light crude oil (Gippsland). The following range of conditions were covered: velocity of 0.25 to 0.65 m/s, surface temperature of 180 to 260°C, bulk temperature of 80 to 120°C, and pressure from 379 to 655 kPa.

Table 3. Summary of operating conditions for Gippsland oil.

| Run # | $T_b$ (°C) | $T_{s,o}$ (°C) | u (m/s) | P (kPa) | Initial $dR_f/dt$ ($m^2K/kJ$) |
|---|---|---|---|---|---|
| 26 | 77 | 245 | 0.35 | 379 | 3.06E-07 |
| 29 | 101 | 253 | 0.35 | 517 | 3.61E-07 |
| 32 | 115 | 252 | 0.35 | 655 | 5.28E-07 |
| 33 | 78 | 243 | 0.35 | 379 | 3.12E-07 |
| 41 | 77 | 242 | 0.40 | 379 | 2.22E-07 |
| 42 | 76 | 247 | 0.30 | 379 | 4.17E-07 |
| 43 | 77 | 249 | 0.25 | 379 | 5.08E-07 |
| 44 | 79 | 177 | 0.25 | 379 | 1.94E-07 |
| 45 | 78 | 196 | 0.25 | 379 | 2.78E-07 |
| 46 | 80 | 217 | 0.25 | 379 | 3.89E-07 |
| 47 | 81 | 259 | 0.25 | 379 | 5.89E-07 |
| 48 | 78 | 249 | 0.25 | 517 | 5.28E-07 |
| 49 | 81 | 251 | 0.25 | 655 | 5.83E-07 |

No fouling was detected using milder operating conditions or at higher velocities, perhaps due to the low asphaltene, ash and sulfur content in Gippsland crude oil.

Fouling runs were carried out for periods of up to 90 hours. An example of typical results is shown in Figure 1, in which heat flux (q), probe surface temperature ($T_s$), bulk fluid temperature ($T_b$), film heat transfer coefficient (U), and thermal resistance (1/U) are plotted with time. Calculations were done according to equations (1) to (4).

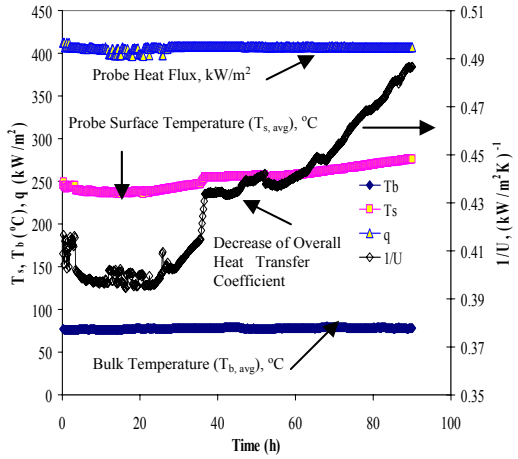


Figure 1. Typical results of a fouling run, velocity of 0.35 m/s, heat flux of 400 kW/$m^2$, bulk temperature of 80°C, initial surface temperature of 240°C, pressure of 379 kPa.

Following an unsteady state period of 3-4 hrs at the beginning of the run, the heat flux and the bulk fluid temperature remain constant within the limits of experimental error. After an induction period of 24 hours, 1/U increased from 0.4 to 0.49 $m^2$K/kW over 90 hours. A pulse type change in $T_s$ and 1/U occurred at time 36 to 38 hrs, possibly due to slight changes in system pressure and fluid flow rate. This fouling run for Gippsland oil was repeated and results are shown in Figure 2. The initial clean coefficients of both runs were very close (2.43 and 2.47 kW/$m^2$K). After 90 hours of operation, the final coefficients were 2.06 and 2.09, a difference of less than 2%. The probe surface temperature increased by 31°C. The initial fouling rates were reproduced within ±4%.

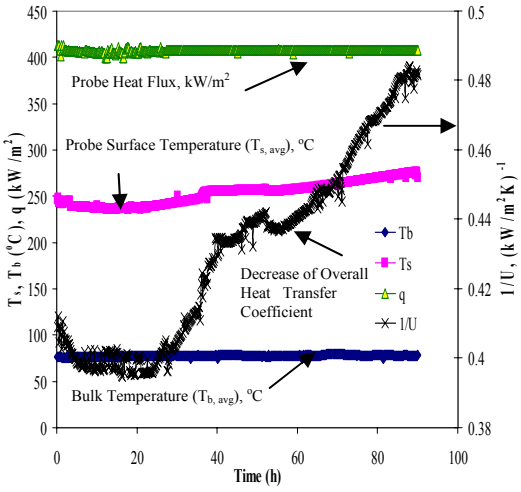


Figure 2. Results of fouling Run 33 to reproduce Run 26 in Figure 1.

Recirculation of test fluid, which results in long periods of heating, may alter fluid composition, and result in differences between the fouling results obtained. Therefore, it was essential to examine the properties (i.e. density, viscosity) of the fluid before and after the fouling runs as presented in Table 4. Changes in properties were found to be negligible.

Table 4. Viscosity and density of Gippsland crude oil measured at the beginning and end of 90-hour fouling runs at T = 30°C.

| Run # | ρ (kg/m$^3$) | ρ (kg/m$^3$) | μ (Pa.s) | μ (Pa.s) |
|---|---|---|---|---|
| | Before run | After run | Before run | After run |
| 26 | 792 | 793 | 1.96E-03 | 2.0E-03 |
| 33 | 792 | 794 | 1.96E-03 | 1.99E-03 |

### 3.1 Effect of Initial Surface Temperature and Heat Flux

Initial surface temperature was varied over the range 180 to 260°C, at a fixed velocity of 0.25 m/s. A fresh batch of fluid was used in each of the runs. It was not possible to go over the limit of 260°C initial surface temperature due to the feed flow rate and the limited probe power. The heat flux fluctuated slightly at the beginning of each experiment, but remained almost constant over the remaining course of the experiment. Attempts were made to keep the variation in bulk temperature to a possible minimum. For this set of runs bulk temperatures were 80°C ± 5.

Figure 3 shows the fouling resistances versus time for Gippsland oil at five different initial surface temperatures.

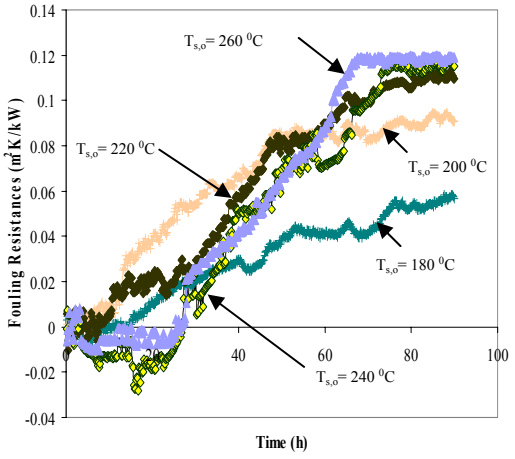


Figure 3. Effect of initial surface temperature on fouling resistance, at $T_b$ = 80°C, velocity = 0.25 m/s, pressure of 379 kPa.

There was an induction period and negative fouling resistances up to 24 hrs, especially at high initial surface temperatures (240, 260°C). These negative resistances were due to the rapid (early) formation of rough deposits, which increased the film heat transfer coefficient.

At an initial surface temperature of 180°C, the probe surface temperature increases with time by about 12°C over the 90 hours of the test, as a result of a small extent of fouling. The heat transfer coefficient decreased with time by about 11% from 2.02 to 1.81 kW/m$^2$K, and appeared to reach an asymptotic value after 75 hrs.

At an initial surface temperature of 260°C, the probe surface temperature increased with time by about 48°C over the 90 hours of the test as a result of fouling. The heat transfer coefficient decreased with time by about 21.7% from 2.32 to 1.82 kW/m$^2$K, and appeared to reach an asymptotic value after 70 hrs.

Rates were calculated from the linear portion of the $R_f$ versus t curves. Fouling rates were most intensive at highest initial surface temperature. Where $R_f$ exceeded 0.08 m$^2$K/kW, asymptotic behavior was apparent, possibly due to a low concentration of fouling precursors left in the oil. A decrease in suspended solids concentration from the initial value of 0.239% was observed when fouling was significant. As initial surface temperature was raised from 180°C to260 °C, the final suspended solids concentration decreased from 0.239% to 0.196%. Increasing the heat flux increased the fouling rate. Fouling rates ranged from 1.94E-07 m$^2$K/kJ at $T_{s,o}$ of 180°C to 5.89E-07 m$^2$K/kJ at $T_{s,o}$ of 260°C. The low extent of fouling may be due to the low asphaltenes concentration in the crude oil.

### 3.2 Effect of Bulk Temperature

Figure 4 show fouling resistance versus time results for three experiments at inlet bulk temperatures of 80, 100 and 120°C, with fixed initial surface temperature, pressure and velocity. At the highest bulk temperature, fouling started to be rapid and severe after about 20 hrs of induction period, reaching $R_f$ values of 0.08 m$^2$K/kW in about 50 hours. Although there is considerable scatter, the trend of fouling with bulk temperature is evident. For $T_b$=80°C, negative $R_f$ values were obtained over the first 32 hours. It was found that if the apparatus was not completely cleaned between experiments, the induction time would decrease.

By increasing the bulk temperature from 80 to 120°C, and hence the film temperature from 163 to 183°C, the fouling rate was increased from 3.06E-07 to 5.28E-07 m$^2$K/kJ. Table 5

shows the percentages of insoluble material measured by hot filtration through a 3-micron filter at 85°C. Over the course of the run, the insoluble material decreased and the extent of the decrease paralleled the fouling rate. Hence, it appears that fouling is related to the presence of insoluble material in the oil.

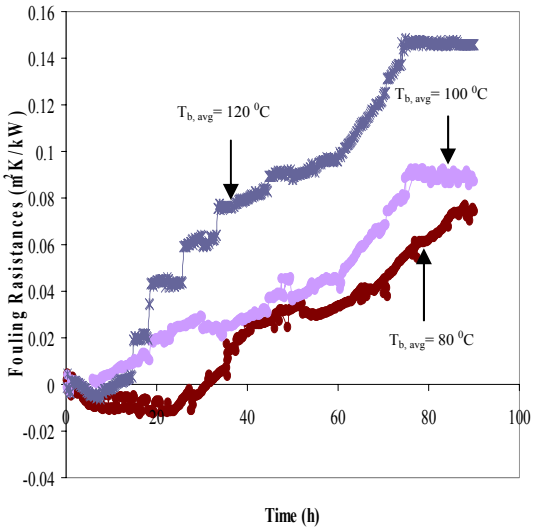


Figure 4. Effect of bulk temperature on fouling resistance, $T_{so}$ = 245°C, velocity = 0.35 m/s, pressure = 379 kPa.

Table 5. Effect of bulk temperature on initial and final concentration of solids.

| $T_b$, °C | Feed Sample | 80 | 100 | 120 |
|---|---|---|---|---|
| wt% | 0.239 | 0.230 | 0.229 | 0.208 |

### 3.3 Effect of Bulk Velocity

Velocity effects provide a key to understanding the fouling mechanism. If fouling rates increase with velocity, transport of fouling species is likely important. If fouling rate decreases with increasing velocity the dominant step is likely to be adhesion of foulants at the surface or chemical reaction.

Figure 5 shows fouling resistance results of experiments carried out at fixed inlet bulk temperature of 80°C, initial surface temperature of 240°C, pressure of 379kPa, and velocities of 0.25, 0.3, 0.35, 0.4 and 0.45 m/s.

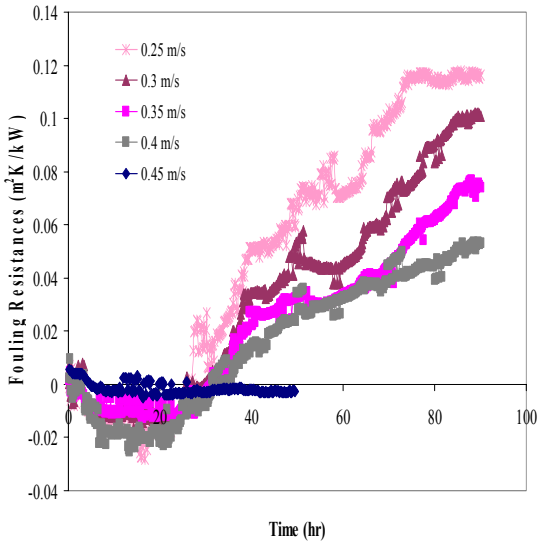


Figure 5. Effect of bulk velocity on fouling resistance, $T_{so}$ = 245°C, $T_b$ = 80°C, pressure = 379 kPa.

At a velocity of 0.25 m/s, the heat transfer coefficient decreased around 20% from 2.17 to 1.74 kW/m²K, while at a velocity of 0.4 m/s, the heat transfer coefficient decreased by 12% over the 90 hrs run. The scatter in $R_f$ during the initial 5 hours is likely due to the non-steady state effects.

Velocity effects at constant surface temperature could be studied over only a narrow range due the power limitation of the fouling probe. As the velocity was raised from 0.25 to 0.4 m/s, the fouling rate decreased by a factor greater than 2; from 5.08E-07 m²K/kJ at a velocity of 0.25 m/s to 2.22E-07 m²K/kJ at a velocity of 0.4 m/s.

No fouling was detected over 50 hours at a velocity of 0.45 m/s as shown in Figure 5. Induction periods up to 24 hours were observed for all runs. A significant decrease in the suspended solids content was noted over each run. Where fouling rate was highest, the decrease was largest.

### 3.4 Effect of Pressure

The pressure effect was investigated in the range of 379 to 655 kPa using nitrogen and at a bulk temperature of 80°C, initial surface temperature of 240°C and a velocity of 0.25 m/s. The tank was purged with nitrogen prior to each run. Results of fouling resistances versus time are shown in Figure 6. The final fouling resistances after 92 hours were 0.12 ± 0.02 m²·K/kW.

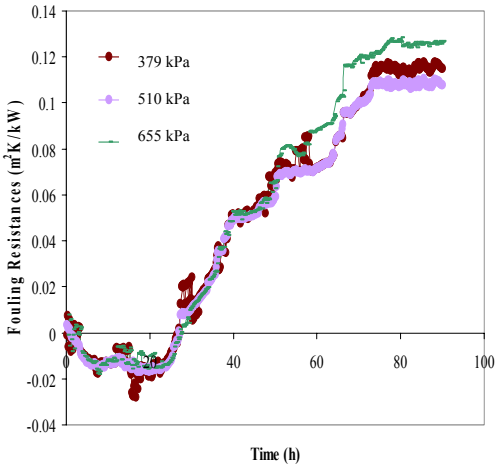


Figure 6. Effect of pressure on fouling resistance, $T_{so}$ = 245°C, $T_b$ = 80°C, velocity = 0.25 m/s.

Results show that over this narrow range, the pressure has a minimal effect on fouling tendency. Increasing the pressure from 379 to 510 kPa increased the initial fouling rate by around 4% from 5.08E-07 to 5.27E-07 $m^2$.K/kJ, while increasing the pressure from 510 kPa to 655 kPa increased the initial fouling rate by around 10% more from 5.27E-07 to 5.83E-07 $m^2$K/kJ. These differences in rate are close to the value of the reproducibility of the fouling rate, hence the pressure effects differences may not be statistically significant.

### 3.5 Correlation of Results

Observations of fouling rates showed a relatively strong effect of surface temperature, a strong effect of bulk temperature, a small effect of pressure and a decrease in fouling rate as velocity was raised (at fixed initial wall temperature). These observations suggest that the deposition of the precursors which may be present increases with bulk temperature, and that both adhesion and the transport of foulants may be important. Fouling appears to be caused by fine solids from the feed material. Physical examination of the fouling probe showed that attachment of these solids was limited to the heated parts of the unit, which is consistent with the surface temperature effect.

An Arrhenius type equation has been used to determine an activation energy based on the film and surface temperatures.

$$\frac{dR_f}{dt} = Ae^{\left(\frac{-E}{RT}\right)} \qquad (8)$$

From the plot of '$\ln[dR_f/dt]$' vs. '$1/T_{s,o}$' or '$1/T_{f,o}$', the slope of the plot is '–E/R', from which the value of the global activation energy can be obtained. The value of the activation energy was higher based on the film temperature (42 kJ/mol) than that based on the surface temperature (28.5 kJ/mol).

The initial fouling rates measured from two sets of experiments were regressed. The first set was conducted at constant $T_{s,o}$ of 240°C, velocity of 0.35 m/s and $T_b$ of 80, 100 and 120°C. The second set was conducted at a constant $T_b$ of 80°C, velocity of 0.25 m/s and $T_{s,o}$ of 180, 200, 220, 240 and 260°C. Results were fitted using a power law equation (Eq. 9) and a Mat Lab program was used to determine the power law exponents:

$$\frac{dR_f}{dt} = A_o P^m u^n e^{-E/RT_{f,o}} \qquad (9)$$

The velocity exponent (n) was -1.43; pressure exponent (m) was 0.18 and the power law constant ($A_o$) was 9.46E-04. The small value of exponent, m, in Eq. 9, reflects the minor effect of P as discussed above. Figure 7 show that the initial film temperature correlates the data well.

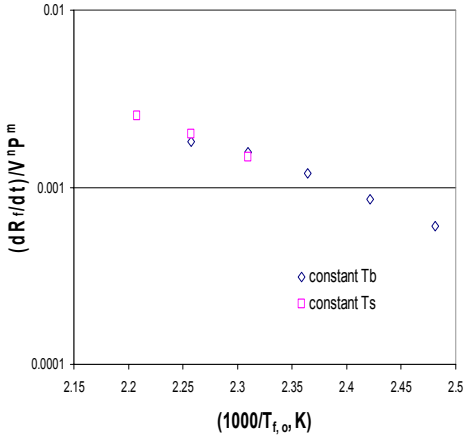


Figure 7. Arrhenius type plot of initial fouling rate vs. initial film temperature.

Results were also fitted to the Ebert and Panchal model (Eq. 7) as shown in Figure 8. The wall shear stress was almost constant around 0.45 ± 0.05 N/$m^2$ for the current runs and the range of film Reynolds number ($Re_{film}$) was 2500 to 4500. The range of film temperatures studied was 131-182°C.

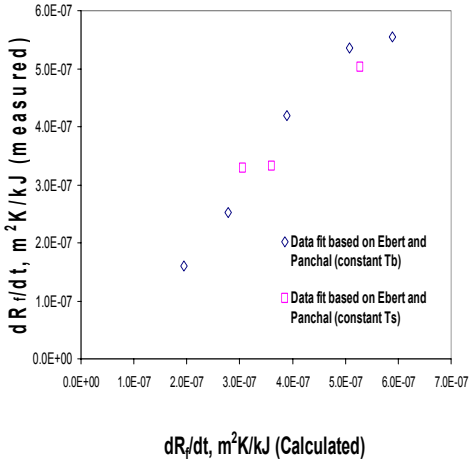


Figure 8. Fit of experimental data to Equation 7.

The resulting values of the four constants were $\alpha = 3.3 \times 10^{6}$ K $m^2$/kJ, $\beta = -0.3$, E = 42.01 kJ/mol, $\gamma = 1.45 \times 10^{-8}$ $m^2$/N (K $m^2$/kJ). The Ebert and Panchal model based on film temperature was consistent with the current data.

### 3.6 Deposit Analysis:

The deposit which built up as the run proceeded appeared as a thin black layer of carbonaceous material on the surface of the probe. SEM micrographs show clusters of agglomerations of asphaltene-like structures that have undergone some form of chemical change on the hot probe surface (see Figure 9).

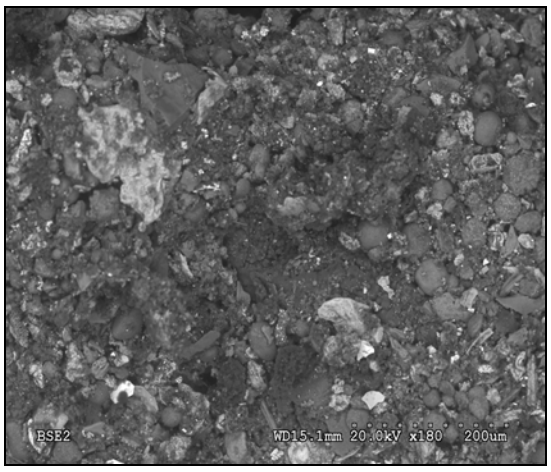


Figure 9. Probe deposit morphology under SEM.

Deposits were collected at the end of each run after photographing the probe. Elemental analyses were performed for some deposit samples and results are presented in Tables 6 and 7. Chemical analysis of collected deposits (Table 6) show the H/C atomic ratio is in the range 1.07 – 1.41 and averaged 1.26, nitrogen content was <0.3 – 0.42% and the sulphur content 2.26-2.99%.

Table 6. Deposit analysis for C, H, N, and S.

| Run # | C (wt%) | H (wt%) | N (wt%) | S (wt%) | Atomic ratio (H/C) |
|---|---|---|---|---|---|
| 26 | 76.5 | 7.8 | <0.3 | 2.99 | 1.22 |
| 32 | 76.61 | 8.44 | <0.3 | 2.26 | 1.32 |
| 42 | 77.51 | 7.96 | 0.42 | 2.47 | 1.23 |
| 43 | 86.97 | 7.76 | 0.33 | 2.78 | 1.07 |
| 46 | 78.30 | 8.56 | 0.30 | 2.48 | 1.31 |
| 49 | 77.60 | 9.16 | 0.37 | 2.48 | 1.41 |

Unaccounted for material, which averaged 11.4% for 5 of the 6 samples is probably mineral matter (ash) and organic oxygen. It is noted that sulphur is highly concentrated in the deposit with % S (deposit) / % S (oil) ≈ 21.

Fouling deposits were further studied using the scanning electron microscope (SEM) along with energy dispersion x-ray (EDX). The EDX analyzer is attached to the SEM to examine the deposit for the presence of elements at the surface using carbon as the standard. The EDX analysis shows the presence of C, O, Cu, Fe and S in the surface structure of Gippsland deposits. Results are shown in Table 7. Oxygen content averaged 9% and Iron content averaged 0.8%. The high copper contents of deposits from runs 32 and 47 are inexplicable.

Table 7. Surface analysis for Gippsland deposits by EDX.

| Run # | C (wt%) | O (wt%) | S (wt%) | Fe (wt%) | Cu (wt%) |
|---|---|---|---|---|---|
| 26 | 87.14 | 8.32 | 2.46 | 0.45 | 0.09 |
| 32 | 82.67 | 8.87 | 3.03 | 1.89 | 3.55 |
| 47 | 83.36 | 9.11 | 2.98 | 1.07 | 3.48 |
| 44 | 89.48 | 8.73 | 1.79 | - | - |

## 4. CONCLUSIONS

A study of fouling of re-circulated Gippsland crude oil led to the following conclusions.

Surface temperature was found to have a major impact on fouling rates. An increase of roughly 80°C results in tripling of the initial fouling rate. Fouling rates for this crude were in the range 2 to 6 x $10^{-7}$ $m^2$K/kJ. Induction times for some of the runs were long and variable.

The fouling rate increased by about 60% with increases in the bulk temperature from 80°C up

to 120°C. This observed bulk temperature effect can not be separated from the flow effects, since as the bulk temperature increases, the Reynolds number goes up slightly at fixed velocity.

The presence of filterable solids means fouling is likely. Increases in fouling rate paralleled decreases in the amount of filterable insolubles in the oil, which was measured at the end of each fouling run. Deposit ash plus oxygen levels by difference were about 11%. The atomic H/C ratio of deposits from all the runs is fairly similar, with a value close to 1.2, which indicates that the solids are mostly composed of aromatics.

Experiments at film Reynolds numbers 2500 – 4500, showed that increased bulk velocities result in decreased fouling rates. Increasing the velocity from 0.25 m/s to 0.4 m/s reduced the fouling rate by a factor of 2. Fouling was undetectable after almost 50 hours, for bulk velocities over 0.4 m/s.

The current data is consistent with a threshold-fouling model based on film temperatures. The range of film temperature involved is 131 – 182°C.

## 5. ACKNOWLEDGEMENTS

Financial support of the Australian Research Council and Caltex Oil Company (NSW, AUSTRALIA) is gratefully acknowledged.

## 6. NOMENCLATURE

| | |
|---|---|
| A | pre-exponential constant, $m^2$.K/kJ |
| $d_{a,o}$, $d_{a,i}$ | annular diameter;outer;inner, mm |
| $d_h$ | hydraulic diameter, mm |
| E | global activation energy, kJ/mol |
| Nu | Nusselt number, dimensionless |
| P | Pressure, kPa |
| Pr | Prandtl number, dimensionless |
| q | heat flux, kW/$m^2$ |
| R | universal gas constant, J/mol.K |
| $R_f$ | fouling resistance, $m^2$K/kW |
| Re | Reynolds number, dimensionless |
| t | time, h |
| $T_b$ | bulk temperature, K or °C |
| $T_f$ | film temperature, K or °C = 0.5($T_s$+$T_b$) |
| $T_{f,o}$ | initial film temperature, K or °C |
| $T_{s,o}$ | initial surface temperature, K or °C |
| U | overall heat transfer coefficient kW/$m^2$K |
| $U_o$ | clean heat transfer coefficient kW/$m^2$K |
| u | fluid velocity, m/s |
| $\lambda$ | thermal conductivity, kW/m.K |
| $\mu$ | dynamic viscosity, Pa.s |
| $\rho$ | density, kg/$m^3$ |
| $\alpha$, $\beta$, $\gamma$ | constants for Ebert and Panchal correlation |
| $\tau$ | wall shear stress, N/$m^2$ |
| EDX | energy dispersion x-ray |
| HTRI | Heat Transfer Research Institute |
| PFRU | portable fouling research unit |
| SEM | scanning electron microscope |

## 7. REFERENCES

Bott, T. R., 1995, Chapter 3 "The Cost of Fouling", in Fouling of Heat Exchangers, Elsevier, B.V., Amsterdam, The Netherlands.

Dickakian, G. B., 1997, The Role of Asphaltene and Polars in Thermal Fouling of Hydrocarbons, Pre-print, Eng. Foundation Conference, Proc. Understanding Heat Exchanger Fouling and its Mitigation, Lucca, Italy.

Ebert, W. A. and Panchal, C. B., 1995, Analysis of Exxon Crude Oil Slip-Stream Coking Data, 'Fouling Mitigation of Industrial Exchange Equipment', Begell House, NY, pp451-460.

Gnielinski, V. 1995, A New Method to Calculate Heat Transfer in the Transition Region between Laminar and Turbulent Tube Flow., Inst. Thermische Verfahrenstech., Univ. Karlsruhe, Germany, Forschung im Ingenieurwesen, 61(9), 240-8. Journal written in German.

Lambourn, G. A. and Durrieu, M., 1983, Fouling in Crude Oil Preheat Trains, in Heat Exchangers-Theory and Practice, Taborek, Hewitt and Afgan (Eds.) Hemisphere, NY. p841-852.

Murphy, G. and Campbell, J., 1992, Fouling in Refinery Heat Exchangers: Causes, Effects, Measurements and Control, in Fouling Mechanisms, M. Bohnet et al. (eds.) 249-261, GREThh Seminar, Grenoble.